Identification of Forest Structure Changes from L-Band SAR Data: A Tomographic Perspective

Matteo Pardini, Noelia Romero-Puig, Roman Guliaev, Konstantinos P. Papathanassiou
German Aerospace Center (DLR), Microwaves and Radar Institute (HR), Wessling, Germany

Abstract

The objective of this work is to investigate the possibility of separating, quantifying and characterizing individual structural / dielectric change contributions occurring in forest stands provided by tomographic SAR acquisitions at different times. This analysis is carried out by processing real multi-temporal L-band tomographic data over a temperate forest in the south of Germany. Different types of structural changes are firstly identified by means of high resolution lidar acquisitions. Their mapping into both tomographic reflectivity reconstructions and related structure indices is then derived. Reasons for ambiguities are discussed.

1 Introduction

L-band Synthetic Aperture Radar (SAR) pulses can penetrate even through dense vegetation layers until the ground, and thus interact with vegetation elements (depending on frequency, polarization and dielectric properties) located at different heights. A set of SAR images acquired under slightly different angular directions along displaced tracks or orbits is required to reconstruct the 3D distribution of the backscattered power, also called reflectivity, and constitutes the measurement principle of interferometric and tomographic SAR (TomoSAR) measurements [1].

Several experimental analyses have demonstrated that TomoSAR reconstructions at different times are sensitive to changes of both forest geometric structure (induced by growth, management, logging, mortality, disturbance, etc.) and dielectric properties (induced by rainfall, droughts, seasonality, etc.) [2]-[5], which can occur simultaneously. However, the parameterization of physical changes of different types and intensities in terms of reflectivity changes, together with the assessment of the possibility to separate, quantify and characterize the individual structural / dielectric change contributions in a time series of TomoSAR acquisitions are critical missing aspects. This results into interpretation ambiguities of the spatial gradients and the temporal changes of the reconstructions in terms of physical processes. Systematic analyses of appropriate change data sets, as well as the development of dedicated models and methodologies are thus required.

The objective of this work is to contribute to fill this gap by investigating the capability of L-band TomoSAR acquisitions to identify specific forest structure changes. This assessment is carried out by considering both TomoSAR reflectivity reconstructions and available structure indices derived from them. The results of this characterization will be used to evaluate the presence of interpretation ambiguities, but also to discuss on the role of the TomoSAR configuration (especially in terms of the vertical resolution) and on the need to adapt different structure indices to the TomoSAR case or even to develop new ones with a larger sensitivity to changes.

2 Structure estimation from TomoSAR profiles

The usual TomoSAR processing obtains 3D reflectivity by reconstructing vertical profiles along the height direction z. In this work, this operation is performed by means of the Capon beamforming [6]. Its vertical resolution is less constrained by the acquisition geometry than a Fourier beamforming, but radiometric linearity might be lost for unfavourable TomoSAR configurations (irregular track displacements and / or poor vertical resolution). For fixed range-azimuth coordinate and polarization channel, the pixel amplitudes in the K images of the TomoSAR set are collected in the K-dimensional vector $\mathbf{y}$. The associated covariance matrix is $\mathbf{R} := E\{\mathbf{y}\mathbf{y}^H\}$, where $E\{.\}$ indicates the statistical expectation operator. In practice, $\mathbf{R}$ is obtained by means of a multi-look averaging operation across multiple adjacent pixels within a cell. The Capon reconstruction of the vertical reflectivity profile $P(z)$ along height corresponding to $\mathbf{R}$ is [6]

$$P(z) = \mathbf{h}^H(z)\mathbf{R}\mathbf{h}(z), \text{ with } \mathbf{h} = \frac{\bar{\mathbf{R}}^{-1}\mathbf{a}(z)}{\mathbf{a}^H(z)\bar{\mathbf{R}}^{-1}\mathbf{a}(z)} \qquad (1)$$

where $\mathbf{a}(z)$ is the steering vector, $\bar{\mathbf{R}}$ is a diagonally loaded version of $\mathbf{R}$, and $(.)^H$ denotes the Hermitian (transpose conjugate operator). The steering vector contains the height-dependent phase (difference) with respect to a generic z for each track. Its $k-$th ($k = 1, \dots, K$) element is $[\mathbf{a}(z)]_k = \exp(jk_{z,k}z)$ where $k_{z,k}$ is the vertical wavenumber associated to the $k-$th image with respect to a reference track [6].

In a recent work [7], forest structural 3-D heterogeneity has been expressed by two indices in the horizontal and vertical direction. Their definition is based on the spatial distribution of the (meaningful) peaks in TomoSAR profiles between ground and canopy top within a structure cell on ground. In particular, the heterogeneity in the horizontal

direction can be inferred by evaluating canopy height variations [8]-[11]. In a TomoSAR framework, this corresponds to evaluate the number of profile peaks in a top canopy layer. Accordingly, let $\mathcal{P} = \{p_1, p_2, \dots, p_P\}$ be the ensemble of the P peaks in the structure cell (excluding the ground peaks). A horizontal structure index HS can be defined as [7]:

$$HS \coloneqq \frac{n(\mathcal{P}_{top})}{A} \tag{2}$$

where $n(\mathcal{P}_{top})$ is the number of elements of a subset $\mathcal{P}_{top}$ of $\mathcal{P}$ constituted by all the peaks with height in the top (vegetation) layer, and A is the area of the structure cell. The top layer corresponds to the range of heights above $\varepsilon \cdot \max(\mathcal{Z})$, where $\varepsilon < 1$ is a usually empirically defined factor (here fixed to 0.6 according to [5], [7]), and $\mathcal{Z}$ is the M-dimensional ensemble of the unique heights corresponding to $\mathcal{P}$. For the same top layer width, a large(r) number of peaks increases HS, indicating a more homogeneous stand. Conversely, a lower number of peaks reduces HS, indicating a more heterogenous stand. It is worth noting that the experiments in [7] demonstrated the close correlation of HS with the well-established stand density index and thus with basal area. For this reason, large(r) values of HS indicate denser(r) stands, while low(er) values indicate sparse(r) stands. A vertical structure index VS can be defined as

$$VS \coloneqq M \operatorname{var}\{\mathcal{Z}\} \tag{3}$$

where $\operatorname{var}\{\mathcal{Z}\}$ is the variance of the peak heights in $\mathcal{Z}$. VS increasing to 1 corresponds to increasing vertical heterogeneity.

3 Data evaluation

3.1 Test site and data sets

The Froschham test site is located in the South of Germany over an essentially flat topography around 590 m above sea level. Canopy heights reach 40 m. Several management activities are being carried out in order to transform even-aged monospecies stands into uneven-aged mixed species stands with a reduction of forest volumes.

The DLR's airborne F-SAR system has been acquiring L-band data over the Froschham site since 2016 within the TempoSAR campaign. In particular, two data sets acquired in May 2017 and May 2023 were selected for the analyses in this work as both allow high vertical resolution analyses. Two fine-beam lidar acquisitions were carried out in 2016 and 2022, and are used to infer the occurring type of structural change of the vegetation elements.

The two TomoSAR sets are both composed by a total of 8 tracks realizing nominal horizontal displacements from 5 m up to 50 m with respect to the reference track. Considering a flight height of around 3000 m above the mean site height, these displacements lead to a vertical TomoSAR resolution of around 7 m within the area of interest delimited by white rectangle in **Figure 1**. The changes occurring in this area are representative for the changes occurring on the whole site.

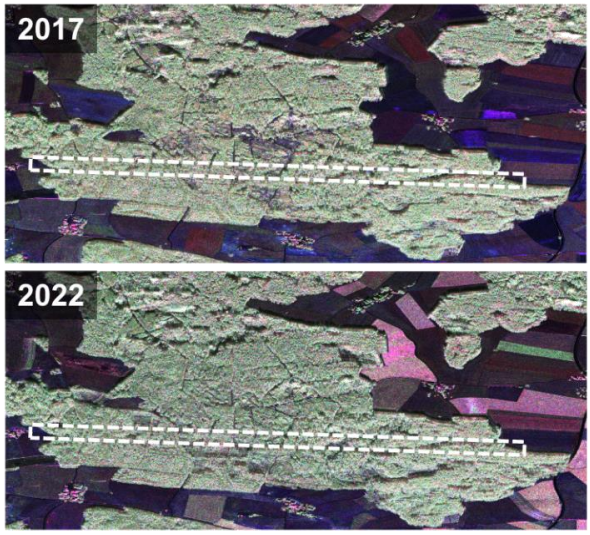

Figure 1 F-SAR RGB Pauli image compositions over the Froschham site. The white rectangle delimits the area where the analyses are focused. The azimuth axis is along the horizontal direction.

3.2 Results

Figure 1 shows the RGB Pauli image compositions for the two sets. A few structure changes in the 5-year time difference are already apparent, especially some regrowth at image center and clear-cuts e.g. closer to the image bottom.

A better identification of those changes on ground which are not well visible in intensity images is enabled by the available lidar acquisitions. **Figure 2** shows the canopy height models (CHM's, i.e. the first return above the ground) for both lidar acquisitions with a resolution of 1 m × 1 m for the white rectangle denoted in **Figure 1**. **Figure 3** reports the Beamforming profiles for the two selected F-SAR sets calculated in the HV channel with a multi-look cell of 25 m × 25 m (azimuth – ground range) at the center of the area of interest in the white rectangle of **Figure 2**. The values of HS and VS calculated within 50 m × 50 m structure cells are plotted in **Figure 4** and in **Figure 5**, respectively. HS and VS have been calculated according to equations (2) and (3) from both TomoSAR Capon and lidar profiles at 5 m × 5 m resolution. Lidar profiles have been derived as the histograms in height of all the returns (return count in every height bin).

A visual evaluation of the CHM in **Figure 2** shows an increasing height from left to right, corresponding to an increasing structural heterogeneity as confirmed by ground measurements. The acquisition times sample changes induced by the management practices. In particular, 5 areas can be individuated, and are denoted with the letters A-E in **Figures 2-5**. The corresponding changes of the Capon reflectivity profiles in **Figure 3** and of the structure indices in **Figure 4 and 5** for both lidar and TomoSAR data are discussed in the following.

In area A, a systematic thinning is recognizable. The ground reflectivity increases in 2023 with respect to 2017 especially where the thinning becomes more intense (larger CHM gaps). It might be interpreted as a consequence of an easier penetration induced by the increase of (top canopy) sparsity. This is consistent with a reduction of the lidar HS, but not with the increase of the TomoSAR HS, which would denote an increase of density. It is likely that in this case a change of dielectric properties has made top-canopy TomoSAR peaks more "visible" in 2023 (as supported by the Capon-reconstructed profiles), thus biasing the change of HS. A less intense thinning (utmost right part of area A) causes no significant change of both the lidar and the TomoSAR HS. No significant changes are visible for VS (as it is reasonable to expect), with substantial agreement between lidar and TomoSAR.

Area B is dominated by clear cuts occurred in the sampled time period. Correspondingly, in 2023 the Capon-reconstructed ground reflectivity increases significantly as it reasonable to expect due to the reduced presence of vegetation. This is also reflected in the decrease of both HS and VS. In this case, there is a rather good agreement between the lidar and TomoSAR structure indices.

Growth of small stands of 5-10 m height is visible in Area C. According to the lidar data, structure indices should not change. TomoSAR data show an increase of HS in 2023 with respect to 2017. The increase of height might have favored the detection of profile peaks in the top canopy layer, hence causing the change in HS.

In area D, some of the taller trees have been cut, although not according to a systematic spatial pattern as the thinning in area A. There is a certain correlation between increase of the reference lidar HS and decrease of the ground reflectivity as a result of the increase of density induced by growth. But such (relatively small) increases may not be fully represented by the TomoSAR HS. Otherwise, the TomoSAR HS and VS agree rather well with the lidar ones. This agreement continues in area E, where essentially no structure change is observable. Interestingly, it has been

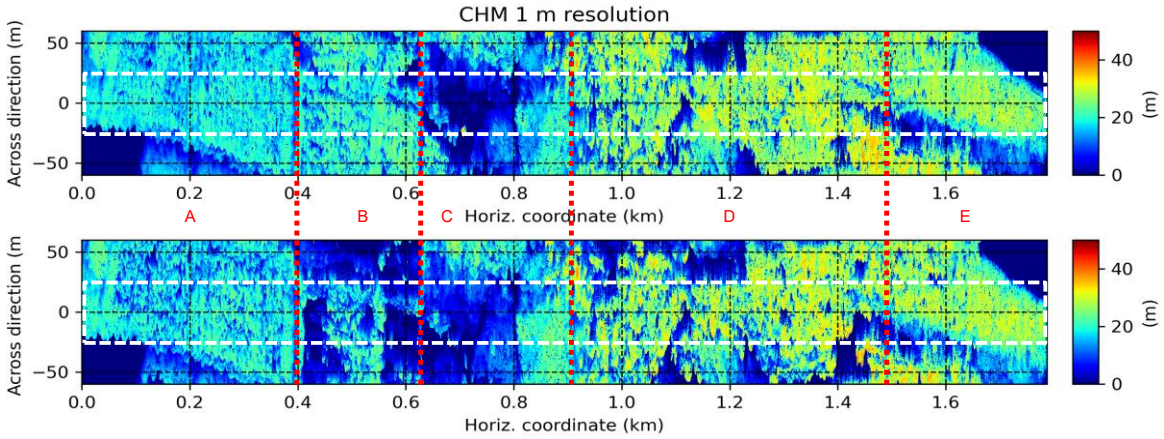

Figure 2 Lidar canopy height maps above ground at 1 m resolution projected in SAR coordinates acquired in 2016 (top panel) and in 2022 (bottom panel). The white dashed rectangles indicate the area used for the structure analysis.

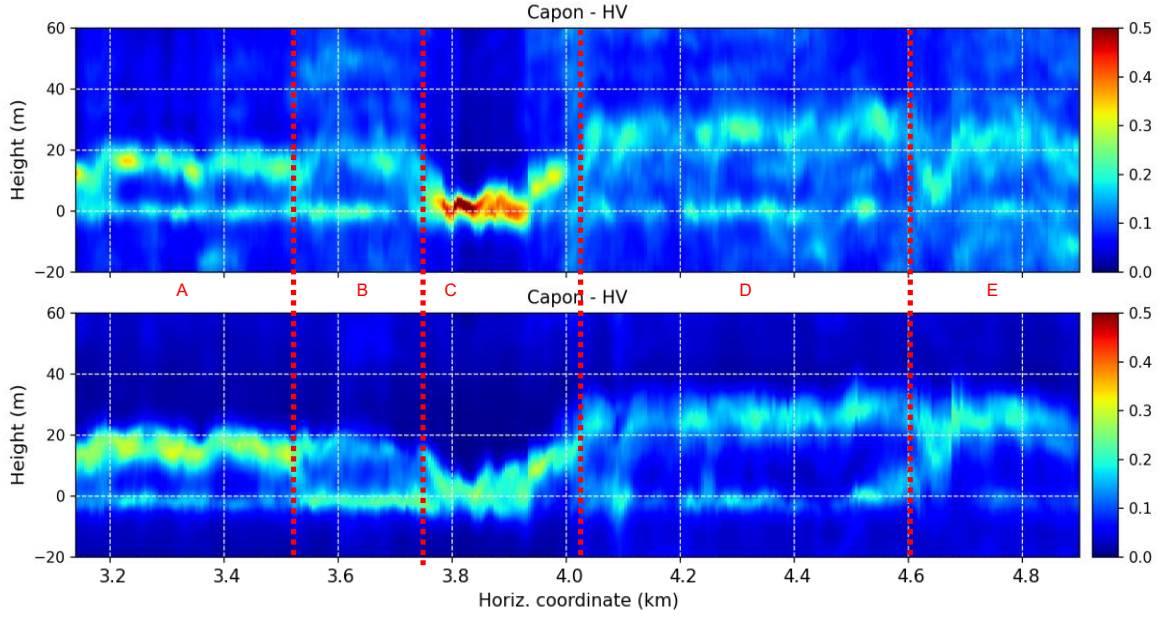

Figure 3 Capon beamforming profiles in HV estimated at 5 m resolution (multi-look cell in ground range) along the center of the white dashed rectangle in Figure 2 for the F-SAR acquisitions of 2017 (top panel), and 2022 (bottom panel).

verified that both lidar and TomoSAR *VS* in area E are smaller than in area D as a result of a less significant understory vegetation.

4 Outlook

The real data results reported in Section 3 confirm that physical forest structure changes indeed effect changes in both the reconstructed reflectivity profiles and in two structur indices expressing horizontal and vertical heterogeneity, confirming previous investigations. The index values calculated from TomoSAR profiles reflect the spatial gradients shown by those calculated from lidar data at both dates. A certain correlation has been found between changes of horizontal structure and changes of ground-to-volume ratios induced mainly by changes of the ground reflectivity. However, the horizontal structure index derived from TomoSAR data might be locally affected by a bias induced by dielectric changes and / or limitations in vertical resolution. This bias can become significant in the evaluation of changes as it can lead to interpretation ambiguities, especially for (relatively) small changes. From these

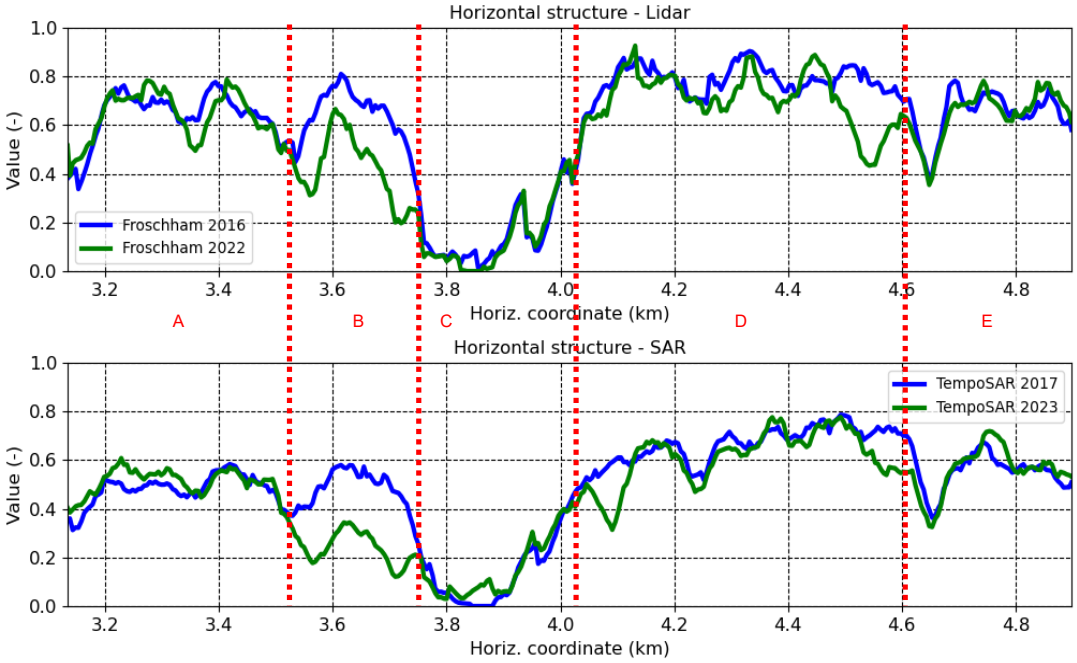

Figure 4 Horizontal structure index calculated by aggregating all TomoSAR and lidar profiles within structure cells of 50 m × 50 m (white dashed rectangle in Figure 2) for the area of interest denoted in Figure 1 .

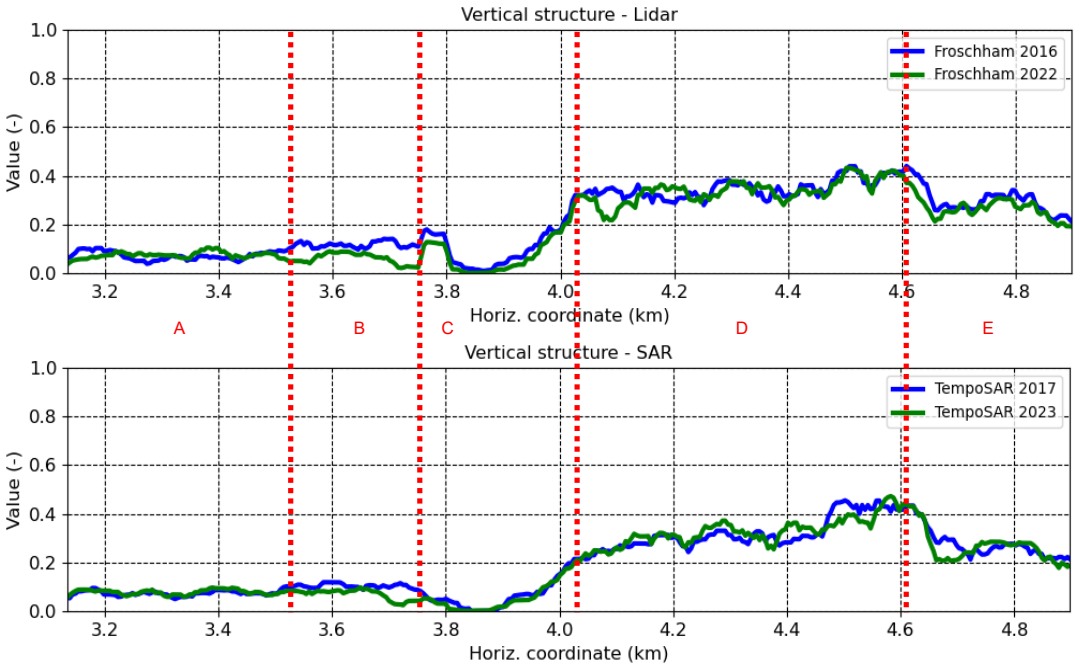

Figure 5 Vertical structure index calculated by aggregating all TomoSAR and lidar within structure cells of 50 m × 50 m (white dashed rectangle in Figure 2) for the area of interest denoted in Figure 1.

results, investigating possibilities to separate between dielectric and structural changes is a critical next step. If achieved, structure indices might restore their capability to interpret correctly reflectivity profile changes in structural terms.

5 Literature

[1] A. Moreira, P. Prats-Iraola, M. Younis, G. Krieger, I. Hajnsek, K. P. Papathanassiou, "A Tutorial on Synthet-ic Aperture Radar," IEEE Geoscience and Remote Sensing Magazine, vol. 1, no. 1, pp. 6-43, Mar. 2013.

[2] V. Cazcarra-Bes, M. Tello-Alonso, R. Fischer, M. Heym, K. Papathanassiou, "Monitoring of Forest Structure Dynamics by Means of L-Band SAR Tomography," Remote Sensing, vol. 9, no. 12, p. 1229, Nov. 2017.

[3] M. Pardini, K. Papathanassiou, F. Lombardini, "Impact of Dielectric Changes on L-Band 3-D SAR Reflectivity Profiles of Forest Volumes," IEEE Transactions on Geoscience and Remote Sensing, vol. 56, no. 12, pp. 7324-7337, Dec. 2018

[4] Y. Bai, S. Tebaldini, D. H. T. Minh, W. Yang, "An Em-pirical Study on the Impact of Changing Weather Conditions on Repeat-Pass SAR Tomography," IEEE Journal of Selected Topics in Applied Earth Observations and Remote Sensing, vol. 11, no. 10, pp. 3505-3511, Oct. 2018.

[5] M. Pardini, V. Cazcarra-Bes, and K. P. Papathanassiou, "TomoSAR Mapping of 3D Forest Structure: Contributions of L-Band Configurations," Remote Sensing, vol. 13, no. 12, p. 2255, Jun. 2021

[6] V. Cazcarra-Bes, M. Pardini, M. Tello, K. P. Papathanassiou, "Comparison of Tomographic SAR Reflectivity Reconstruction Algorithms for Forest Applications at L-band," in IEEE Transactions on Geosci-ence and Remote Sensing, vol. 58, no. 1, pp. 147-164, Jan. 2020.

[7] M. Tello, V. Cazcarra-Bes, M. Pardini, K. Papathanassiou, "Forest Structure Characterization From SAR Tomography at L-Band," in IEEE Journal of Selected Topics in Applied Earth Observations and Remote Sensing, vol. 11, no. 10, pp. 3402-3414, Oct. 2018.

[8] P. Couteron, P. Pelissier, E. Nicolini, D. Paget, "Predicting tropical forest stand structure parameters from Fourier transform of very high-resolution remotely sensed canopy images," Journal of Applied Ecology, 42: 1121-1128, 2005.

[9] C. Carabajal, D. Harding, "RTM C-Band and ICESat Laser Altimetry Elevation Comparisons as a Function of Tree Cover and Relief," Photogrammetric Engineering & Remote Sensing, vol. 12, no. 3, pp. 287-298, Mar. 2006.

[10] M. Neumann, S. S. Saatchi, D. B. Clark, "Quantifying spatial and temporal dynamics of tropical forest structure using high resolution airborne lidar," 2012 IEEE International Geoscience and Remote Sensing Symposium, Munich, Germany, 2012, pp. 1664-1667.

[11] E. De Grandi, E. Mitchard, D. Hoekman, "Wavelet Based Analysis of TanDEM-X and LiDAR DEMs across a Tropical Vegetation Heterogeneity Gradient Driven by Fire Disturbance in Indonesia," Remote Sensing, vol. 8, no. 8, p. 641, Aug. 2016.